Block-Ordered Layered Detector for MIMO-STBC Using Joint Eigen-Beamformers and Ad-Hoc Power Discrimination Scheme

Won Cheol Lee

Abstract: **Suitable for multi-input multi-output (MIMO) communications, the joint beamforming space-time block coding (JBSTBC) scheme is proposed for high-speed downlink transmission. The major functionality of the scheme entails space-time block encoder and joint transmit and receive eigen-beamformer (EBF) incorporating with block-ordered layered decoder (BOLD), and its operating principle is described in this paper. Within these functionalities, the joint EBFs will be utilized for decorrelating fading channels to cause an enhancement in the spatial diversity gain. Furthermore, to fortify the capability of layered successive interference cancellation (LSIC) in block-ordered layered decoding process, this paper will develop a simple ad-hoc transmit power discrimination scheme (TPDS) based on a particular power discrimination function (PDF). To confirm the superior behavior of the proposed JB-STBC scheme employing ad-hoc TPDS, computer simulations will be conducted under various channel conditions with the provision of detailed mathematical derivations for clarifying its functionality.**

Index Terms: **Eigen-beamformer (EBF), layered interference cancellation, linear precoding, multiple-input multiple-output (MIMO) systems, orthogonal space-time block coding (OSTBC).**

I. INTRODUCTION

Towards a further increase in throughput, high spectral efficiency under frequency resource and transmission power restrictions is strongly required. So far, promising multiple-input multiple-output (MIMO) systems have been exploited for future mobile system applications. Among them, the Bell Labs layered space-time (BLAST) scheme developed by Foschini *et al.* [1] has gained a great deal of attraction due to its potential to increase the capacity over the wireless link by a factor of the minimum of the number of receive and transmit antennas. Furthermore, for the receiver corresponding to BLAST-type of multi-substream transmission, many sophisticated signal processing algorithms, such as the near-optimal sphere decoding [2], and minimum mean squared error (MMSE) receiver combined with layered successive interference cancellation (LSIC) [1] have been introduced.

To invoke the spatial diversity in MIMO systems, various types of space-time block coding (STBC) schemes for multiple transmit and receive antennas have been considered in [3]–[5]. Specially, in [4], it is proved that a complex orthogonal design and the corresponding STBC which provides full-diversity and full-rate, i.e., the code rate is one, is not possible for more than two antennas. Thus, for more than two antennas, the code rate turns out to be less than one of nature, and whose possible upper bound for generalized complex orthogonal STBC has been discussed in [6]. Moreover, due to the redundant transmission having code rate less than one, the symbol mapper should have higher constellation sizes in order to keep the transmission symbol rate as well as the source bit rate unchanged. To withstand the performance degradation arising from the usage of high-constellation, the quasi-orthogonal STBC (QSTBC) was introduced which yields full-rate and half-diversity [7] or full-diversity [8]. Furthermore, the result in [9] showed that full-diversity space-time codes such as orthogonal STBC (OSTBC) extract the maximum diversity gain achievable without channel state information (CSI) at the transmitter in presence of spatial correlation.

However, despite the numerous affirmative features brought by the usage of MIMO systems, the correlation between MIMO channels leads to a loss in capacity [10]–[12]. In [13], authors mentioned that a potential capacity even beyond the one possible for independent fading may be offered by taking advantage of fading correlation made possible by the transmitter. Specifically, the performance of OSTBC over correlated channels deteriorates rapidly with increasing channel correlation due to the lack of diversity gain. As a solution of this dilemma, it has been already revealed in [3], [14], and [15] that the eigen-beamformer (EBF) in the notion of linear precoding (linear transformation) process has been utilized so as to result in superior performances at low signal-to-noise ratio (SNR) or highly correlated MIMO channels. Recently, many researches have been accomplished to obtain the optimal precoding (transformation) matrix in the sense of minimizing the pairwise error probability upon the usage of OSTBC in multiple-input single-output (MISO) or MIMO systems [3], [15]–[18]. Generally, the optimal linear precoder comprises of two major functionalities with having channel correlation feedback such that eigenbeamforming forces transmission only on a nonzero eigenmodes and power allocation pours the appropriate powers on specific eigenmodes by using waterfilling method as shown in [3], [15], [17], and [19].

The major contribution of this paper can be categorized into two parts. The first is to exploit an efficient scheme for OSTBC-based multi-substream transmission as a form of precoded spatial multiplexing in presence of spatial channel correlation. Towards this, the transmit EBF and ad-hoc power allocation deployable to transmit spatially multiplexed substreams are considered agreeing with the notion of linear precoder such as the method introduced in [20]. Moreover, in proposed receiver

Manuscript received October 28, 2003; approved for publication by Jinho Choi, Division II Editor, May 9, 2006.

W. C. Lee is with the School of Electronic Engineering, Soongsil University, Seoul, Korea, email: wlee@ssu.ac.kr.

structure, along the recovery of multiple substreams, simple decoding process such as the maximum ratio combining (MRC) is used concatenated by block-ordered layered decoder (BOLD) carrying out LSIC rather than complicated MMSE or zero forcing (ZF) detector. To provide the robustness along LSIC process, this paper introduces a sub-optimal power allocation based on ad-hoc transmit power discrimination scheme (TPDS).

This paper is organized as follows. Section II briefly investigates and discusses the validity of the MIMO matrix channel model utilized in this paper. Section III addresses the functionality of the joint beamforming space-time block coding (JBSTBC) whose receiver is equipped with BOLD for STBC (BOLD-STBC) for the recovery of spatially multiplexed substreams in an appropriate order determined by inspecting received block-wise SINRs. Section IV proposes and explains the TPDS obeying the power discrimination function (PDF) proposed in this paper. In Section V, the proposed JBSTBC will undergo a performance evaluation via computer simulations. Section VI provides discussions and conclusions.

II. PARAMETRIC MIMO CHANNEL MODELING

The MIMO channel between M_t transmit and M_r receive antennas is constituted of $M_t \times M_r$ distinct propagation paths arising in pairs of transmit and receive antennas. Provided that multiple wireless channels experience flat fading, the transmit and receive spatial covariance matrices denoted by $\mathbf{R}_t$ and $\mathbf{R}_r$, respectively, which are characterized in terms of the profile of departure and arrival angle spread and the geometric configuration of antenna array. Each element in spatial covariance matrix reads the degree of mutual correlation between individual fading channel parameters.

The MIMO channel shown can be expressed in terms of $M_r \times M_t$ matrix as the following

$$\mathbf{H} \triangleq \left[\mathbf{h}_1\ \mathbf{h}_2 \cdots \mathbf{h}_{M_t}\right] \tag{1}$$

where $\mathbf{h}_i = [h_{i,1}\ h_{i,2}\ \cdots\ h_{i,M_r}]^T$, $i = 1, \cdots, M_t$, and $h_{i,j}$ indicates the channel parameter invoked in downlink path between the i-th transmit antenna and the j-th receive antenna, and superscript T means the transposition. Assume that the distance between transmit and receive antenna is far enough, elements of covariance matrix $\mathbf{R}_t$ are distinct upon the geometric location of transmit antennas only. Similarly, elements consisting $\mathbf{R}_r$ are dependent only on the positions of receive antennas. Let us denote the transposition of $\mathbf{H}$ in (1) to be

$$\mathbf{H}^T \triangleq \left[\tilde{\mathbf{h}}_1\ \tilde{\mathbf{h}}_2 \cdots \tilde{\mathbf{h}}_{M_r}\right] \tag{2}$$

where $\tilde{\mathbf{h}}_j = [h_{1,j}\ \ h_{2,j}\ \ \cdots\ \ h_{M_t,j}]^T$, $j = 1, \cdots, M_r$, then with a help of (1) and aforementioned statements, the following relations can be obtained.

$$\mathbf{R}_r \triangleq \mathbf{E}\left\{\mathbf{h}_i\,\mathbf{h}_i^H\right\}, \quad i = 1, \cdots, M_t \tag{3}$$

and

$$\mathbf{R}_t \triangleq \mathbf{E}\left\{\tilde{\mathbf{h}}_j\,\tilde{\mathbf{h}}_j^H\right\}, \quad j = 1, \cdots, M_r \tag{4}$$

where $\mathbf{E}\{\cdot\}$ denotes statistical expectation operator and the superscript H denotes the complex conjugate transposition. And for $M_t = M_r = 4$, these spatial covariance matrices, i.e., $\mathbf{R}_t$ and $\mathbf{R}_r$, can be generally represented in a form of Hermitian toeplitz matrix whose first row is $[1\ a\ b\ c]$, where a, b, and c are the complex valued normalized correlation coefficients.

According to [21]–[23], the MIMO channel as in (1) can be modeled in straightforward as the following

$$\mathbf{H} = \mathbf{R}_r^{1/2}\,\mathbf{G}\,\mathbf{R}_t^{T/2} \tag{5}$$

where the matrix $\mathbf{G}$ of size $M_r \times M_t$ is comprised of identically and independently distributed (i.i.d.) complex Gaussian random variables having zero mean and unit variance. In (5), the half decomposed matrices $\mathbf{R}_t^{1/2}$ and $\mathbf{R}_r^{1/2}$ are expressed in terms of corresponding eigenvectors and root squared eigenvalues, i.e.,

$$\mathbf{R}_r^{1/2} = \mathbf{Q}_r\,\mathbf{\Lambda}_r^{1/2} \text{ and } \mathbf{R}_t^{1/2} = \mathbf{Q}_t\,\mathbf{\Lambda}_t^{1/2} \tag{6}$$

where $\mathbf{Q}_t$ and $\mathbf{Q}_r$ are the collections of eigenvectors relevant to $\mathbf{R}_t$ and $\mathbf{R}_r$, respectively, and the diagonal matrices $\mathbf{\Lambda}_t$ and $\mathbf{\Lambda}_r$ are comprised of corresponding eigenvalues. Upon the parametric matrix channel model in (5), the following relationships can be verified

$$\mathbf{E}\left\{\mathbf{H}\mathbf{H}^H\right\} = M_t\,\mathbf{R}_r \text{ and } \mathbf{E}\left\{\mathbf{H}^T\mathbf{H}^*\right\} = M_r\,\mathbf{R}_t \tag{7}$$

where $()^*$ means the complex conjugation. The above equations can be easily inferred from the intrinsic relationships for transmit and receive covariance matrices shown in (3) and (4).

III. PRINCIPLES OF JBSTBC SCHEME WITH BLOCK-ORDERED SUCCESSIVE DECODING

This section describes the functionality of the JBSTBC scheme proposed in this paper, whose functionality justified as the space-time block encoder and its BOLD incorporated with transmit and receive EBFs. Fig. 1(a) depicts the generic structure of JBSTBC transmitter where the single symbol stream is spatially multiplexed into $N(= M_t/2)$ substreams, then MIMO-STBC encoded individually, and M_t outputs are conveyed into the block of transmit EBF. Fig. 1(b) shows the structure of JB-STBC receiver comprised of a bank of receive EBFs, and a series of BOLD-STBC whose functionality is explained in detail later on. Here in summary, the iterative BOLD-STBC is performed in block-wise based on the inspection of received SINRs at each time. Then, the successive signal separation is proceeded in pre-determined order with using *a priori* detected block of symbols as well as estimates of channel parameters. This procedure is repeated successively until the block of symbols having the lowest SINR is finally recovered. In the sequel, the parallel-to-serial converter multiplexes decoded bit streams to retrieve the original bit sequence.

Let us denote $\mathbf{w}_i$, $i = 1, \cdots, M_t$, as the weight vectors corresponding to transmit EBF, $\mathbf{x} = [x_1\, x_2 \cdots x_{M_t}]^T$ as the output vector after the MIMO-STBC encoder, and $\mathbf{t} = [t_1\, t_2 \cdots t_{M_t}]^T$ as the beamformed vector at the front end. Here, the signal vector $\mathbf{t}$ to be transmitted can be expressed in a form of the weighted linear combination as the following

$$\mathbf{t} = \mathbf{w}_1 x_1 + \mathbf{w}_2 x_2 + \cdots + \mathbf{w}_{M_t} x_{M_t} = \mathbf{W}\mathbf{x} \tag{8}$$

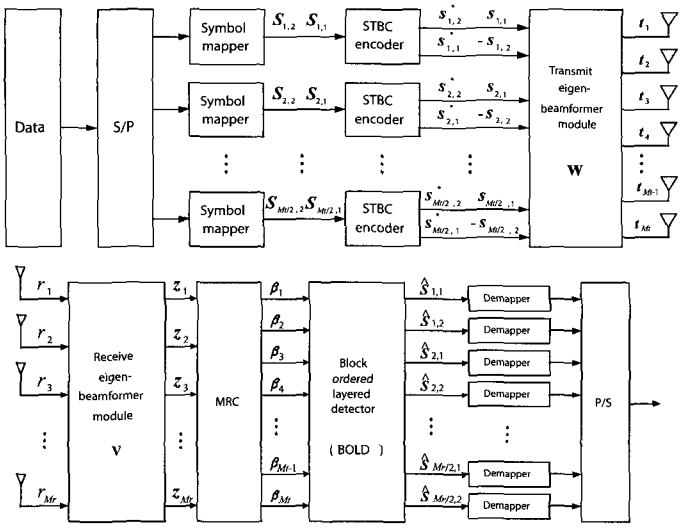

Fig. 1. Block diagrams of JBSTBC transmitter and receiver: (a) Structure of JBSTBC transmitter, b) structure of JBSTBC receiver.

where the matrix $\mathbf{W}$ of size $M_t \times M_t$ is the collection of EBF weight vectors, which are identical to the eigenvectors associated with the transmit covariance matrix $\mathbf{R}_t$, i.e., $\mathbf{w}_i \equiv \mathbf{q}_i^{t*}$, $i = 1, \cdots, M_t$. Thus,

$$\mathbf{W} \equiv \left[\mathbf{q}_1^{t*}\ \mathbf{q}_2^{t*} \cdots \mathbf{q}_{M_t}^{t*}\right] = \mathbf{Q}_t^* . \tag{9}$$

In the sense of maximizing the capacity on the downlink transmission, the optimal strategy is to transmit independent complex Gaussian sequences throughout beamformers whose weight vectors are the eigenvectors of $\mathbf{E}\left\{\mathbf{H}^H\mathbf{H}\right\}$ [16]. According to (7), since these eigenvectors are the same as those of $\mathbf{R}_t$, it can be stated that the usage of transmit eigen-beamfomers purposely meets the notion of increasing MIMO capacity. Similarly, the complex weight vector for receive beamformer denoted by $\mathbf{v}_j$ is identical to the eigenvector of $\mathbf{R}_r$, i.e.,

$$\mathbf{v}_j \equiv \mathbf{q}_j^r , \quad j = 1, \cdots, M_r . \tag{10}$$

By using the parametric MIMO channel model discussed in Section II, the received vector $\mathbf{r} = [r_1\ r_2\ \cdots\ r_{M_r}]^T$ can be expresed in terms of matrix channel modeled in (5), transmitted signal vector $\mathbf{t}$, and additive noise vector $\mathbf{n}$ as the following

$$\mathbf{r} = \mathbf{H}\,\mathbf{t} + \mathbf{n} = \mathbf{R}_r^{1/2}\,\mathbf{G}\,\mathbf{\Lambda}_t^{1/2}\,\mathbf{x} + \mathbf{n} \tag{11}$$

where the noise vector $\mathbf{n}$ is comprised of i.i.d. complex Gaussian random variables with zero mean and variance of $\sigma_n^2 = N_0/2$. Referring to the receiver structure shown in Fig. 1(b), the received vector after the receive beamforming process is denoted by $\mathbf{z} = [\mathbf{z}_1\, \mathbf{z}_2 \cdots \mathbf{z}_{M_r}]^T$ whose explicit expression is

$$\mathbf{z} \triangleq \left[\mathbf{v}_1^H\mathbf{r}\ \ \mathbf{v}_2^H\mathbf{r}\ \cdots\ \mathbf{v}_{M_r}^H\mathbf{r}\right]^T = \tilde{\mathbf{G}}\,\mathbf{x} + \tilde{\mathbf{n}} \tag{12}$$

where $\tilde{\mathbf{G}} = \mathbf{\Lambda}_r^{1/2}\,\mathbf{G}\,\mathbf{\Lambda}_t^{1/2}$ and $\tilde{\mathbf{n}} = \mathbf{Q}_r^H\,\mathbf{n}$ are the modified MIMO channel and noise vector, respectively. With the usage of transmit and receive EBFs, it is worthwhile to mention that the original matrix channel $\mathbf{H}$ is altered to $\tilde{\mathbf{G}}$ whose input and output are $\mathbf{x}$ and $\mathbf{z}$, respectively. Furthermore, since the elements consisting $\tilde{\mathbf{G}}$ are complex Gaussian random variables satisfying i.i.d. characteristic, the modified MIMO channel parameters arising from the usage of joint eigen-beamforemers become completely independent with each other. Accordingly, this could provide the enhancement of the order of spatial diversity. This paper assumes the perfect estimation of elements of the modified matrix channel.

In transmitter depicted in Fig. 1, the consecutive symbols $s_{i,1}$ and $s_{i,2}$ are input to the i-th MIMO-STBC encoder, then 2×2 output symbol matrix are generated from each encoder over two-symbol period. Assume that the channel experiences frequency non-selective slow fading, the consecutive received samples denoted as $z_q(0)$ and $z_q(1)$ received at the q-th antenna over a certain two-symbol period can be expressed as the following

$$\begin{bmatrix} z_q(0) \\ z_q(1) \end{bmatrix} = \sum_{k=1}^{M_t/2} \begin{bmatrix} \frac{s_{k,1}}{\sqrt{2}} & \frac{-s_{k,2}^*}{\sqrt{2}} \\ \frac{s_{k,2}}{\sqrt{2}} & \frac{s_{k,1}^*}{\sqrt{2}} \end{bmatrix} \begin{bmatrix} \tilde{g}_{q,2k-1} \\ \tilde{g}_{q,2k} \end{bmatrix} + \begin{bmatrix} \tilde{n}_q(0) \\ \tilde{n}_q(1) \end{bmatrix} \tag{13}$$

where $\tilde{g}_{i,j}$ indicates the (i,j)-th component of $\tilde{\mathbf{G}}$. To make further progress, rewriting (13) in a vector notation gives rise to

$$\mathbf{z}_q = \sum_{k=1}^{M_t/2} \tilde{\mathbf{G}}_{q,k}\,\mathbf{x}_k + \tilde{\mathbf{n}}_q \tag{14}$$

where

$$\mathbf{z}_q \triangleq [z_q(0)\ \ z_q^*(1)]^T \tag{15}$$

$$\mathbf{x}_k \triangleq \left[s_{k,1}/\sqrt{2}\ \ s_{k,2}^*/\sqrt{2}\right]^T \tag{16}$$

$$\tilde{\mathbf{n}}_q \triangleq [\tilde{n}_q(0)\ \ \tilde{n}_q^*(1)]^T \tag{17}$$

and

$$\tilde{\mathbf{G}}_{q,k} \triangleq \begin{bmatrix} \tilde{g}_{q,2k-1} & -\tilde{g}_{q,2k} \\ \tilde{g}_{q,2k}^* & \tilde{g}_{q,2k-1}^* \end{bmatrix} . \tag{18}$$

In order to perform further decoding process, with using (13)–(15), the following relationship can be constructed.

$$\mathbf{y} = \mathbf{\Theta}\,\mathbf{u} + \boldsymbol{\eta} \tag{19}$$

where

$$\mathbf{y} \triangleq \left[\mathbf{z}_1^T\ \mathbf{z}_2^T\ \cdots\ \mathbf{z}_{M_r}^T\right]^T \tag{20}$$

$$\mathbf{\Theta} \triangleq \left[\tilde{\mathbf{G}}_1\ \tilde{\mathbf{G}}_2\ \cdots\ \tilde{\mathbf{G}}_{M_t/2}\right] \tag{21}$$

$$\mathbf{u} \triangleq \left[\mathbf{x}_1^T\ \mathbf{x}_2^T\ \cdots\ \mathbf{x}_{M_t/2}^T\right]^T \tag{22}$$

$$\boldsymbol{\eta} \triangleq \left[\tilde{\mathbf{n}}_1^T\ \tilde{\mathbf{n}}_2^T\ \cdots\ \tilde{\mathbf{n}}_{M_r}^T\right]^T \tag{23}$$

and

$$\tilde{\mathbf{G}}_k \triangleq \left[\tilde{\mathbf{G}}_{1,k}^T\ \tilde{\mathbf{G}}_{2,k}^T\ \cdots\ \tilde{\mathbf{G}}_{M_r,k}^T\right]^T . \tag{24}$$

As a first step for generating decision statistics for block-ordered JBSTBC decoding, MRC process is preceded on received vector $\mathbf{y}$ with the usage of *a priori* known matrix $\mathbf{\Theta}$ of size $2M_r \times M_t$. As a result,

$$\boldsymbol{\beta} = \mathbf{\Theta}^H\,\mathbf{y} = \mathbf{A}\,\mathbf{u} + \boldsymbol{\xi} \tag{25}$$

where $\boldsymbol{\beta} \triangleq [\boldsymbol{\beta}_1^T \ \boldsymbol{\beta}_2^T \ \cdots \ \boldsymbol{\beta}_{M_t/2}^T]^T$ with $\boldsymbol{\beta}_i \triangleq [\beta_{i,1} \ \beta_{i,2}]^T$ is representing a vector of decision statistics for a series blocks of symbols. And $\boldsymbol{\xi} = \boldsymbol{\Theta}^H \boldsymbol{\eta}$ is the noise vector, and the square matrix $\mathbf{A} = \boldsymbol{\Theta}^H \boldsymbol{\Theta}$ of size $M_t \times M_t$ is denoted as the "characteristic matrix" [5]. Here the matrix $\mathbf{A}$ is composed of $M_t/2 \times M_t/2$ block matrices $\mathbf{A}_{k,l}$, $k, l = 1, \cdots, M_t/2$, whose component matrix can be expressed by

$$\mathbf{A}_{k,l} = \tilde{\mathbf{G}}_k^H \tilde{\mathbf{G}}_l = \sum_{q=1}^{M_r} \mathbf{B}_q^{(k,l)} \tag{26}$$

where $\mathbf{B}_q^{(k,l)}$ is

$$\begin{bmatrix} \tilde{g}_{q,2k-1}^* \tilde{g}_{q,2l-1} + \tilde{g}_{q,2k} \tilde{g}_{q,2l}^* & -\tilde{g}_{q,2k-1}^* \tilde{g}_{q,2l} + \tilde{g}_{q,2k} \tilde{g}_{q,2l-1}^* \\ \tilde{g}_{q,2k-1} \tilde{g}_{q,2l}^* - \tilde{g}_{q,2k}^* \tilde{g}_{q,2l-1} & \tilde{g}_{q,2k-1} \tilde{g}_{q,2l-1}^* + \tilde{g}_{q,2k}^* \tilde{g}_{q,2l} \end{bmatrix} \tag{27}$$

In (27), it can be easily noticed that the off-diagonal component matrix satisfies the orthogonal property due to its intrinsic formation, i.e., $\mathbf{A}_{k,l}\mathbf{A}_{k,l}^H$ or $\mathbf{A}_{k,l}^H\mathbf{A}_{k,l} = \gamma \mathbf{I}_{2\times 2}$ for a specific real number γ. Here, it has been well established in [5] and [24] that the "characteristic matrix" $\mathbf{A}$ in (25) plays a key role of determining the system performance in an average sense. In other words, as long as the values of off-diagonal elements in $\mathbf{E}\{\mathbf{A}\}$ are not trivial, due to the existence of additional substream interference, the resulting performance after the MRC starts to degrade [5]. The optimal performance can be achieved whenever off-diagonal elements of $\mathbf{E}\{\mathbf{A}\}$ are vanished. For the proposed JBSTBC scheme, since $\mathbf{E}\left\{\tilde{g}_{q,k}\, \tilde{g}_{q',k'}^*\right\} = 0$ for either $q \neq q'$ or $k \neq k'$, off-diagonal elements of $\mathbf{A}$ are automatically trivialized in an average sense. This tells us that the proposed JBSTBC scheme gives a possibility of achieving optimal performance in an average sense. In accordance with this observation, the matrix $\mathbf{E}\{\mathbf{A}\}$ can be represented in terms of only diagonal elements, that is

$$\mathbf{E}\{\mathbf{A}\} = diag\left\{\left[\delta_1 \ \delta_2 \ \cdots \ \delta_{M_t/2}\right] \otimes \mathbf{I}_2\right\} \tag{28}$$

where $\delta_k = M_r \left(\lambda_{2k-1}^t + \lambda_{2k}^t\right)$, $k = 1, \cdots, M_t/2$. Referring to (28), the covariance matrix of the noise vector after the MRC denoted as $\boldsymbol{\xi}$ in (25) has the form of a diagonal matrix in an average sense, i.e.,

$$\mathbf{E}\left\{\boldsymbol{\xi}\,\boldsymbol{\xi}^H\right\} = \mathbf{E}\left\{\boldsymbol{\Theta}^H \boldsymbol{\eta}\boldsymbol{\eta}^H \boldsymbol{\Theta}\right\} = \sigma_n^2 \mathbf{E}\{\mathbf{A}\}. \tag{29}$$

With using (25)–(27), the decision statistics $\hat{\mathbf{x}}_k$ for the k-th transmitted block of symbols can be represented as

$$\hat{\mathbf{x}}_k \triangleq \boldsymbol{\beta}_k = \tilde{\mathbf{G}}_k^H \tilde{\mathbf{G}}_k \mathbf{x}_k + \sum_{l=1 \,\&\, l\neq k}^{M_t/2} \tilde{\mathbf{G}}_k^H \tilde{\mathbf{G}}_l \mathbf{x}_l + \boldsymbol{\xi}_k. \tag{30}$$

Assume that the transmitted symbols are independent, and the average signal power is $\sigma_s^2 = \mathbf{E}\left\{|s_{k,1}|^2\right\} = \mathbf{E}\left\{|s_{k,2}|^2\right\}$, referring to (30), the SINRs for $s_{k,1}$ and $s_{k,2}$ are the same. Here, let us denote SINR_k as the block SINR for the symbol vector $\mathbf{x}_k$ defined in (16), it can be represented by

$$\mathrm{SINR}_k = \frac{P_{k,s}}{P_{k.I} + P_{k.N}} \tag{31}$$

where $P_{k,s}$, $P_{k,I}$, and $P_{k,N}$ are signal, interference and noise powers associated with the wanted k-th block of symbol vector $\mathbf{x}_k$, respectively, and those are expressed as

$$P_{k,s} = \left(A_{k,k}^{(1,1)}\right)^2 \frac{\sigma_s^2}{2} = \left(\sum_{q=1}^{M_r} |\tilde{g}_{q,2k-1}|^2 + |\tilde{g}_{q,2k}|^2\right)^2 \frac{\sigma_s^2}{2} \tag{32}$$

$$P_{k,I} = \sum_{l=1 \,\&\, l\neq k}^{M_t/2} \left(\left|A_{k,l}^{(1,1)}\right|^2 + \left|A_{k,l}^{(1,2)}\right|^2\right) \frac{\sigma_s^2}{2} \tag{33}$$

and

$$P_{k,N} = A_{k,k}^{(1,1)}\, \sigma_n^2 = \sum_{q=1}^{M_r} \left(|\tilde{g}_{q,2k-1}|^2 + |\tilde{g}_{q,2k}|^2\right) \sigma_n^2. \tag{34}$$

Referring to (32), the MRC gain arising from MIMO-STBC decoding is $(A_{k,k}^{(1,1)})^2$, equivalently, it has a form of the summation of absolute squared i.i.d. Gaussian random variables. Clearly, this gives an opportunity of improving the order of spatial diversity. Furthermore, it is worthwhile to mention that the values of SINR_k, $k = 1, \cdots, M_t/2$, are distinct with respect only to block index k. The iterative BOLD-STBC process proposed in this paper is performed in block-wise accompanied by sorting out the order of decoding with the inspection of received SINR_k's for every symbol blocks. This is a well-known approach appeared in V-BLAST algorithm [25], [26], such that a successive inter-substream interference cancellation is executed with respect to *a priori* assigned order. Here, the major difference between the BOLD for the proposed JBSTBC and the V-BLAST is originated from the usage of MRC rather than MMSE linear filtering.

Along the successive signal separation procedure, if the deviations among the eigenvalues of transmit covariance matrix are small, it is hard to discriminate the received SINRs. In this situation, it may not be beneficial to the usage of BOLD, so that it is inevitable to experience the unwanted error propagation. In order to mitigate this kind of degradation, this paper proposes the TPDS in the next section which fortifies the capability of successive signal separation.

IV. SUB-OPTIMAL TRANSMIT POWER ALLOCATION USING AD-HOC TRANSMIT POWER DISCRIMINATION SCHEME (TPDS)

In rich scattering environments, since the channels experienced at multiple antennas are likely to be independent, the eigenvalues associated with the spatial covariance matrix are close to the unity with small deviation. Whereas, under the sparse scattering environment, it could be conjectured that the degree of correlation between channels experienced at high-installed antennas becomes considerable. In this case, the deviation among eigenvalues associated with transmit covariance matrix would be significant, so that the eigenvalue spread ratio, i.e., the ratio between the maximum and the minimum eigenvalue, becomes quite large. In addition, referring to (25) and (28), the deviation of received SINRs increases in this situation because the received SINRs are surely dependent on the eigenvalues corresponding to transmit covariance matrix.

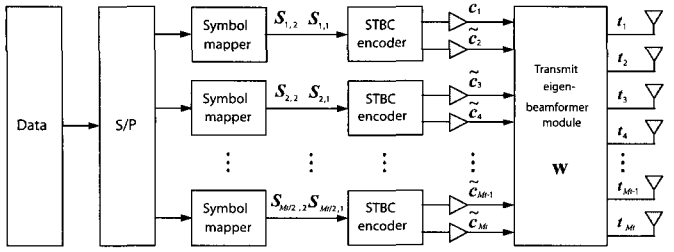

Fig. 2. Structure of modified JBSTBC transmitter with employing transmit power allocation based on ad-hoc TPDS.

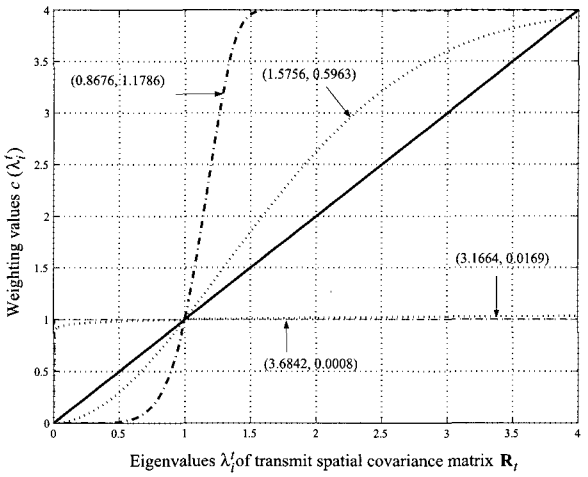

Fig. 3. PDF curves for several different pairs of minimum and maximum eigenvalues.

At the receiver, prior to the recovery of each block-wise symbols using STBC decoder, a decoding order could be arranged with respect to the values of received SINRs. Provided that the depth of correlation between fading channels between all the transmit antennas to any fixed receive antenna, namely *forward channels*, is trivial, eigenvalues of transmit covariance matrix becomes almost unity. This situation implies a lack of deviation among received SINRs, such that SIC conducted during the BOLD process becomes corrupted due to the strong coexistence of inter-substream interferences.

As a modified version of Fig. 1(a), Fig. 2 illustrates a transmitter structure with applying sub-optimal power allocation based on TPDS. Here, extra weighting value denoted by $\tilde{c}_i$, $i = 1, \cdots, M_t$, can be updated via a mapping process on the basis of the proposed PDF. Here, the PDF is a memoryless mapping function whose input is an eigenvalue of transmit spatial covariance matrix and output is an extra weighting value to be applied onto each substream. With the usage of this ad-hoc power allocation, the received SINRs are properly discriminated so as to mitigate any major error propagation occurred in steps for LSIC.

The proposed PDF used for ad-hoc TPDS is expressed as a function of eigenvalue λ_i^t, i.e., for $i = 1, \cdots, M_t$

$$\tilde{c}_i = \frac{c(\lambda_i^t)}{\rho} = \frac{M_t}{\rho}\left[1 - \exp\left\{\alpha\left(\lambda_i^t\right)^{\frac{\mathrm{CO}}{\mathrm{ESR}}}\right\}\right] \tag{35}$$

where "ESR" and "CO" stand for the eigenvalue spread ratio and the curve order, respectively. Here, ESR can be obtained by dividing the maximum eigenvalue by the minimum among λ_i^t, for $i = 1, \cdots, M_t$. In (35), $\alpha = \ln(1 - 1/M_t)$ and $\rho = \sqrt{\sum_{i=1}^{M_t} c^2(\lambda_i^t)/M_t}$. Here ρ is used as a normalization factor to make the total transmit power consistent regardless of the number of transmit antennas. The PDF introduced in (35) has the "*S*-curve" characteristic, whose degree of bending is determined by either ESR or CO. Thus, for a fixed CO, if the ESR approaches infinity, the curve corresponding to $c(\lambda_i^t)$ nearly becomes flat as unity. Otherwise, when ESR is almost unity, curve shows steep "*S*-curve." Here, it is worthwhile to mention that the "*S*-curve" for $c(\lambda_i^t)$ designated by (35) always crosses the unit point $(1, 1)$ no matter what ESR value is brought out. Thus, when the eigenvalues are near unity, i.e., *forward channels* are likely uncorrelated, the values of $c(\lambda_i^t)$, for $i = 1, \cdots, M_t$, are extremely diversified ranging from 0 through M_t due to the intrinsic "*S*-curve" characteristics. Whereas, if *forward channels* are strongly correlated, those become almost unity. The aforementioned PDF is a nonlinear function whose input is ranged from 0 to M_t. This is due to the fact that the eigenvalues of covariance matrix having unit diagonal terms are confined from 0 to M_t at most. Thus, whenever one of eigenvalues is unity, then all the other eigenvalues also become unity. This reads that the *forward channels* are surely perfectly uncorrelated, such that, inherently, the ESR turns out to be unity. Conversely, when one of eigenvalues is M_t, the rest are zeros.

In (35), the CO determines the depth of power discrimination, so that high CO provides heavy discrimination. However, the increase in CO does not always imply the improved performance along the action of LSIC. Since the excessive discrimination is accomplished when the CO is large, this yields erroneous error propagation because a certain SINR associated with specific substream becomes too small. Here, in order to choose an appropriate CO, it would be insightful to exploit the optimization process with the notion of the minimization of error probability such as the averaged bit error rate (BER) behaviors. Towards this, a proper criterion should be realized so as to bring out the exact closed-form solution for choosing optimal CO. Unfortunately, the exact formula is yet to be available at this time, relevant work is under investigation and left as a future study.

Fig. 3 shows shapes of the PDFs before the normalization for several different pairs of minimum and maximum eigenvalues with respect to the CO of 5. Without loss of generality, the number of transmit antenna is set to 4 for this example. In Fig. 3, the abscissa indicates eigenvalue λ_i^t whose values exist in definite between 0 through 4, and the ordinate specifies the corresponding weighting value $c(\lambda_i^t)$ prior to the normalization. There are four distinct PDF curves shown in Fig. 3 with respect to the degree of correlation between channels. Corresponding pairs of minimum and maximum eigenvalues are designated as $(\lambda_{\min}, \lambda_{\max}) = (0.8675,\ 1.1786)$, (1.5756, 0.5963), (3.1664, 0.0169), and (3.6842, 0.0006). The diagonal line in Fig. 3 is used only for reference. As shown in Fig. 3, when the depth of fading correlation is *substantial*, i.e., the eigenvalue spread ratio turns out to be large, all of weighting values are almost unity. This reads the highly correlated situation, since SINRs are already diversified enough, an appropriate block-wise ordering and detection can be accomplished without the help of

ad-hoc power discrimination. Conversely, in presence of *moderate* depth of correlation, due to the intrinsic behavior of the proposed PDF, the difference between allocated transmit powers becomes enlarged. In other words, at low correlation, the weighting values agreeing the notion of transmit power allocation play a role of discriminating received SINRs on purpose so as to enforce LSIC effectively.

In accordance with the weighting values allocated to the transmit antennas, the modified matrix channel in (12) is changed into the following

$$\tilde{\mathbf{G}} \equiv \mathbf{\Lambda}_r^{1/2}\,\mathbf{G}\,\mathbf{\Lambda}_t^{1/2}\,\mathbf{\Sigma}_{\tilde{c}} \tag{36}$$

where $\mathbf{\Sigma}_{\tilde{c}}$ is a diagonal matrix of size $M_t \times M_t$ which is comprised of weighting values calculated based on the employment of PDF, i.e.,

$$\mathbf{\Sigma}_{\tilde{c}} = diag\left[\tilde{c}_1 \;\; \tilde{c}_2 \;\; \cdots \;\; \tilde{c}_{M_t}\right]. \tag{37}$$

Then most of equations below (13) up to (35) are sustained except (28) in which the component matrix after the expectation turns out to be the following

$$\delta_k = M_r\left\{\tilde{c}_{2k-1}^2\lambda_{2k-1}^t + \tilde{c}_{2k}^2\lambda_{2k}^t\right\},\; k=1,\cdots,M_t/2. \tag{38}$$

Upon the aforementioned TPDS is derived in sub-optimal manner, the sequential BOLD-STBC incorporated with the signal separation process begins with inspecting which block among β_k, $k = 1,\cdots,M_t/2$, in (25) produces the highest SINR. In other words, once the index k chosen by using (32)–(34) satisfies $\arg\max_k \mathrm{SINR}_k$, then symbols consisting the selected k-th block are decoded first. If those symbols are perfectly recovered, the new decision statistics vector $\boldsymbol{\beta}^{(1)}$ for decoding next symbol block is updated via proper signal separation, i.e., newly updated vector containing decision statistics can be represented by

$$\boldsymbol{\beta}^{(1)} = \mathbf{A}^{(1)}\,\mathbf{u}^{(1)} + \boldsymbol{\xi}^{(1)} \tag{39}$$

where $\mathbf{A}^{(1)}$ is the matrix of size $(M_t-2)\times(M_t-2)$ constructed by eliminating $(2k-1)$-th and $(2k)$-th rows and columns from $\mathbf{A}$ in (26) and (27), and $\boldsymbol{\beta}^{(1)}$ is the vector of size $(M_t-2)\times 1$ constructed as the following. Let us denote $\mathbf{A}_k$ as the matrix of size $M_t \times 2$ composed of $(2k-1)$-th and $(2k)$-th columns of $\mathbf{A}$ only, at first, subtracting $\mathbf{A}_k\,\mathbf{x}_k$ from $\boldsymbol{\beta}$ gives rise to the vector denoted by $\tilde{\boldsymbol{\beta}}^{(1)}$, and from this vector knocking out $(2k-1)$-th and $(2k)$-th components results in $\boldsymbol{\beta}^{(1)}$. Also in (39), $\mathbf{u}^{(1)}$ and $\boldsymbol{\xi}^{(1)}$ are the residual vectors after excluding the vector $\mathbf{x}_k$ from (22) and $\boldsymbol{\xi}_k$ from the vector $\boldsymbol{\xi}$, respectively. Then, this whole block-ordered decoding process is repeatedly carried out, whose major functionalities are the inspection of the highest SINR among blocks of decision statistics and the procedure of the signal separation. For the 2nd stage of signal separation, the appropriate block index j corresponding to the highest SINR should be chosen by the computation of the following equation, i.e., for $j \neq k$

$$\arg\max_j \left\{\mathrm{SINR}_j^{(1)}\right\}_{j=1}^{M_t/2} \tag{40}$$

Table 1. Successive signal separation steps for BOLD-STBC.

Initialization:
$\boldsymbol{\beta}^{(0)} = \boldsymbol{\beta}$
$\mathbf{A}^{(0)} = \mathbf{A}$

Steps for successive BOLD-STBC:
For $i = 0$ to $M_t/2 - 1$
- Step 1: Determine block index k subject to satisfying $\arg\max_k \mathrm{SINR}_k^{(i)}$
- Step 2: Detect symbols $\hat{\mathbf{x}}_k = [\hat{s}_{k,1}\;\hat{s}_{k,2}]^T$ sliced from the selected block $\boldsymbol{\beta}_k^{(i)}$
- Step 3: Perform signal separation by constructing $\tilde{\boldsymbol{\beta}}^{(i+1)} = \boldsymbol{\beta}^{(i)} - \mathbf{A}_k\,\hat{\mathbf{x}}_k$ upon $\mathbf{A}_k$ and *a priori* detected symbols $\hat{\mathbf{x}}_k$
- Step 4: Update $\boldsymbol{\beta}^{(i+1)}$ for detecting $(i+1)$-th symbol block by taking out elements indexed in $2k-1$ and $2k$ from $\tilde{\boldsymbol{\beta}}^{(i+1)}$

end

where

$$\mathrm{SINR}_j^{(1)} \triangleq \frac{\left(A_{j,j}^{(1,1)}\right)^2}{\sum\limits_{\substack{l=1\\ l\neq j\,\&\,k}}^{M_t/2}\left(\left|A_{j,l}^{(1,1)}\right|^2 + \left|A_{j,l}^{(1,2)}\right|^2\right) + \dfrac{A_{j,j}^{(1,1)}N_0}{\sigma_s^2}}. \tag{41}$$

Again, these whole steps are repeated and finished until the last symbol vector is finally decoded. The flow of steps for the signal separation processes of the BOLD-STBC are summarized in Table 1.

V. SIMULATION RESULTS AND PERFORMANCE ANALYSIS

Whereas this paper introduces the generic structure of the proposed MIMO system as shown in Figs. 1 and 2, the reference model for conducting simulations is its simplified version having 4 transmit and 4 receive antennas although the proposed structure can be more extendable. Assuming the joint beamformers are commonly utilized, as there are more number of transmit antennas, the larger size of matrix should be inverted, so that the amount of computations required for MMSE or ZF based detectors becomes enormous. This may hinder the proper receiving process. However, the proposed receiver utilizes only MRC and BOLD, so that the complexity is relatively not so serious blockage.

To illustrate the performance enhancement, this section provides a series of BER curves and computational complexity of the proposed JBSTBC scheme equipped with BOLD only or BOLD and TPDS together. The results quantify the degree of goodness and reveal the affirmative effects induced by the proposed scheme in presence of fading correlation between MIMO channels. The original bit stream derives into the rate-1/2 convolutional channel coder for QPSK or the rate-1/3 convolutional channel coder for 16-QAM, the block-interleaver and then symbol mapper in sequence.

Referring to [27], four kinds of transmit covariance matrices are considered prescribed as in Table 2, in which PAS, AS, and AOD stand for the power azimuth spectrum, the angle spread,

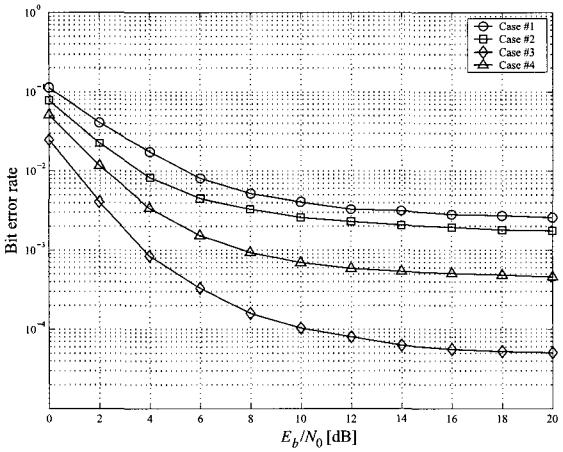

Fig. 4. Performances of BOLD-STBC without employing transmit and receive EBFs (QQPSK modulation).

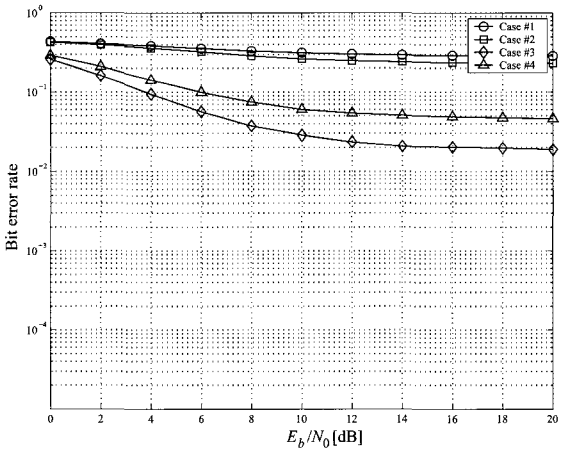

Fig. 5. Performances of BOLD-STBC without employing transmit and receive EBFs (16-QAM modulation).

and the angle of departure, respectively. Here, a, b, and c are normalized correlation coefficients, whose relevant constitution of spatial covariance matrix is already mentioned in Section II. Here in Table 2, the transmit covariance matrix in Case #1 reads the extremely correlated case, whereas, that in Case #4 represents the weakly correlated case. For the receiver, the antenna spacing is 0.5 times the carrier wavelength, uniform PAS over 360° and 0° angles of arrival in every case. This yields $a = -0.30$, $b = 0.22$, $c = -0.18$ [27], which designate strongly correlated channels. In our simulations, the perfect covariance feedback is presumed without involving delay and error.

A. Performance of BOLD-STBC in MIMO Systems without Eigen-Beamformers

According to the description of parametric MIMO channel as in (5), the performance of the BOLD-STBC decoding scheme without employing joint eigen-beamfomers is verified by changing the depth of fading correlations. Figs. 4 and 5 show the BER behaviors with respect to given E_b/N_0's. The overall decoding and signal separation processes follow the steps shown in Table 1. Here, the "characteristic matrix" $\mathbf{A}$ are comprised

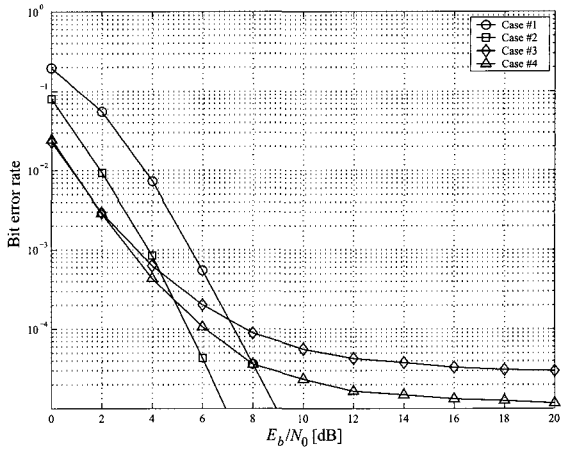

Fig. 6. Performance of the proposed JBSTBC equipped with BOLD (QPSK modulation).

of pure channel parameters synthesized from the parametric MIMO channel model as in (5), whose component matrices, i.e., $\mathbf{A}_{k,l}$, $k,l = 1,\cdots,M_t/2$, are described as the following

$$\mathbf{A}_{k,l} = \sum_{q=1}^{M_r} \mathbf{B}_q^{(k,l)} \tag{42}$$

where $\mathbf{B}_q^{(k,l)}$ is

$$\begin{bmatrix} h_{q,2k-1}^* h_{q,2l-1} + h_{q,2k} h_{q,2l}^* & -h_{q,2k-1}^* h_{q,2l} + h_{q,2k} h_{q,2l-1}^* \\ h_{q,2k-1} h_{q,2l}^* - h_{q,2k}^* h_{q,2l-1} & h_{q,2k-1} h_{q,2l-1}^* + h_{q,2k}^* h_{q,2l} \end{bmatrix}. \tag{43}$$

And the vector of decision statistics has the same form as in (25) in which the noise vector $\xi \equiv \Theta^H \mathbf{n}$ is expressed as the following

$$\boldsymbol{\xi} = \begin{bmatrix} \tilde{\mathbf{G}}_{1,1} & \tilde{\mathbf{G}}_{1,2} & \cdots & \tilde{\mathbf{G}}_{1,M_t/2} \\ \tilde{\mathbf{G}}_{2,1} & \tilde{\mathbf{G}}_{2,2} & \cdots & \tilde{\mathbf{G}}_{2,M_t/2} \\ \vdots & \vdots & \ddots & \vdots \\ \tilde{\mathbf{G}}_{M_t/2,1} & \tilde{\mathbf{G}}_{M_t/2,2} & \cdots & \tilde{\mathbf{G}}_{M_t/2,M_t/2} \end{bmatrix} \begin{bmatrix} \mathbf{n}_1 \\ \mathbf{n}_2 \\ \vdots \\ \mathbf{n}_{M_t/2} \end{bmatrix} \tag{44}$$

where

$$\tilde{\mathbf{G}}_{q,k} = \begin{bmatrix} h_{q,2k-1} & -h_{q,2k} \\ h_{q,2k}^* & h_{q,2k-1}^* \end{bmatrix} \text{ and } \mathbf{n}_q = \begin{bmatrix} n_q(0) \\ n_q^*(1) \end{bmatrix}. \tag{45}$$

Clearly, it is a noticeable fact that the increase in the level of correlation degrades the BER performance due to the loss of diversity gain. To overcome this deterioration, together with using BOLD scheme, the joint eigen-beamformers will be used. And the next subsection shows the evolution in performance.

B. Performance of the Proposed JBSTBC-BOLD

As mentioned earlier, the joint EBFs installed at both transmitter and receiver work for removing inherent fading correlations so as to increase the order of spatial diversity. Figs. 6 and 7 show the BER behaviors resulted from conducting the BOLD-STBC combined with joint EBF without involving the proposed TPDS.

Table 2. Parameters for transmit spatial covariance matrices.

	Case #1	Case #2	Case #3	Case #4
PAS	Laplacian	Laplacian	Laplacian	Laplacian
Topology	0.5λ	0.5λ	4λ	4λ
AS	$15°$	$20°$	$10°$	$15°$
AoD	$2°$	$10°$	$50°$	$-20°$
Spatial covariance matrix	$a = 0.77 + 0.08i$ $b = 0.41 + 0.09i$ $c = 0.22 + 0.08i$	$a = 0.57 + 0.35i$ $b = 0.11 + 0.26i$ $c = -0.01 + 0.16i$	$a = 0.15 + 0.09i$ $b = 0.03 + 0.03i$ $c = 0.00 + 0.01i$	$a = -0.03 - 0.03i$ $b = 0.00 - 0.02i$ $c = -0.48 + 0.40i$

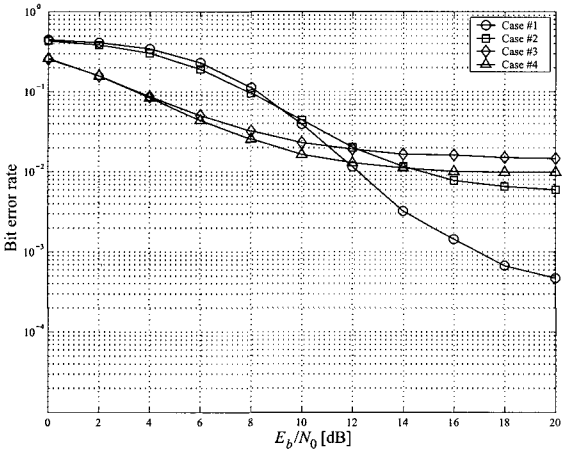

Fig. 7. Performance of the proposed JBSTBC equipped with BOLD (16-QAM modulation).

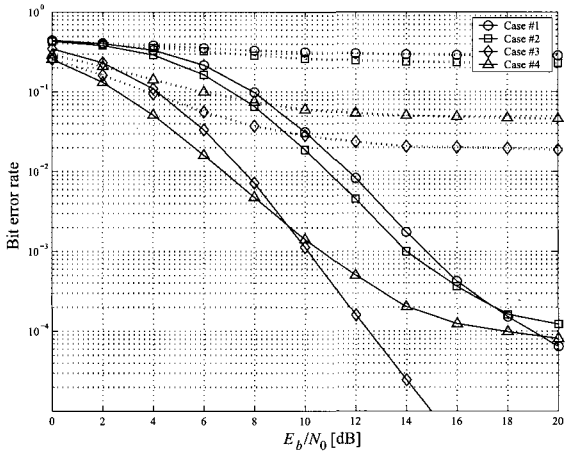

Fig. 9. Performance of JBSTBC-BOLD using TPDS based on the proposed PDF having CO of 6 (16-QAM modulation).

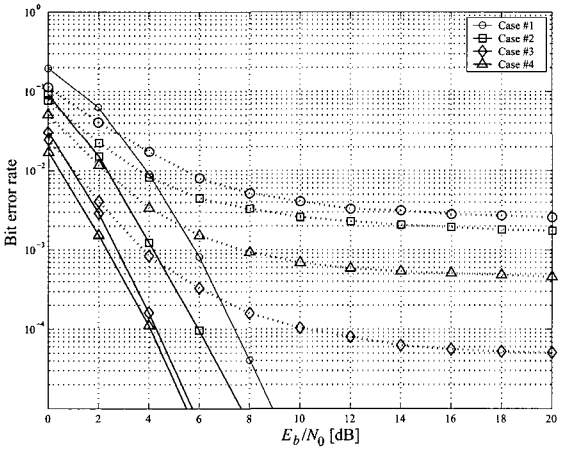

Fig. 8. Performance of JBSTBC-BOLD using TPDS based on the proposed PDF having CO of 3 (QPSK modulation).

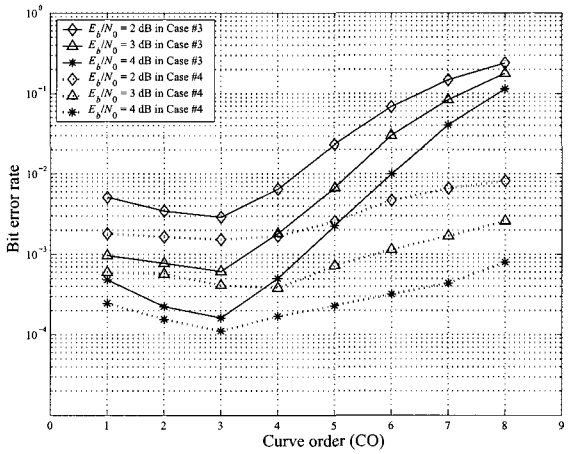

Fig. 10. Average BER performances upon the selection of integer-valued curve order for Cases #3 and #4.

According to the BER curves revealed in Figs. 6 and 7, for the cases when the fading correlation is relatively strong (Cases #1 and #2), plausible performances could be obtained. However, in the existence of weak correlations (Cases #3 and #4), only a little performance improvement is evident regardless of employing EBFs. The performance improvement in highly correlated cases is attributed to enhanced successive encoding process due to the increased power difference between desired signals and interference. This increase is exclusively brought along by the usage of transmit eigen-beamformer. However, in low correlated cases, regardless of the transmit eigen-beamformer, the relatively strong interferences exist, and it may cause the hindrance along the successive signal separation. Alternatively speaking, the minor improvement in weakly correlated situation is emanated from the insignificant deviations between received SINRs corresponding to multiple substreams, consequently, the serious error propagation could occur in the execution of LSIC. To make a further progress, the proposed TPDS based on PDF will be deployed, whose results will be exploited in next subsection.

C. *Performance of JBSTBC-BOLD Combined with TPDS Based on PDF*

As discussed in previous subsection, in case of relatively low correlation, the performance of the proposed JBSTBC employing the BOLD scheme is not satisfactory due to the existence

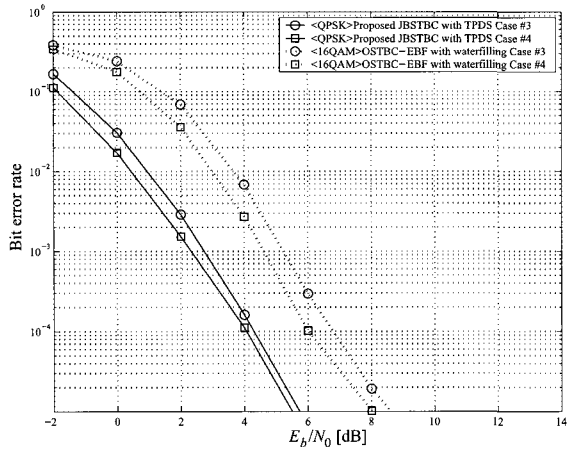

Fig. 11. Performance of JBSTBC-BOLD using TPDS for QPSK modulation compared with OSTBC using precoding scheme.

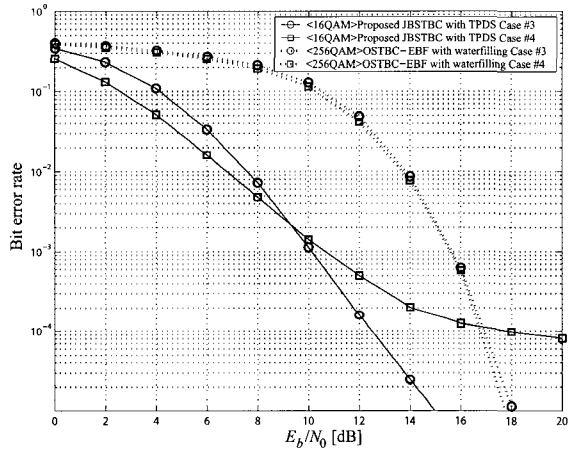

Fig. 12. Performance of JBSTBC-BOLD using TPDS for 16-QAM modulation compared with OSTBC using precoding scheme.

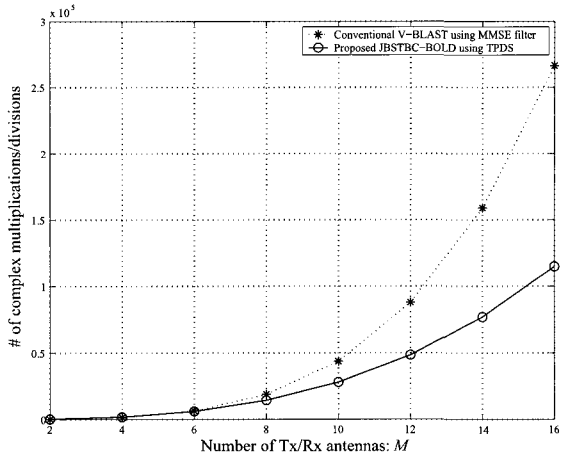

Fig. 13. Number of complex multiplications/divisions vs number of Tx/Rx antennas.

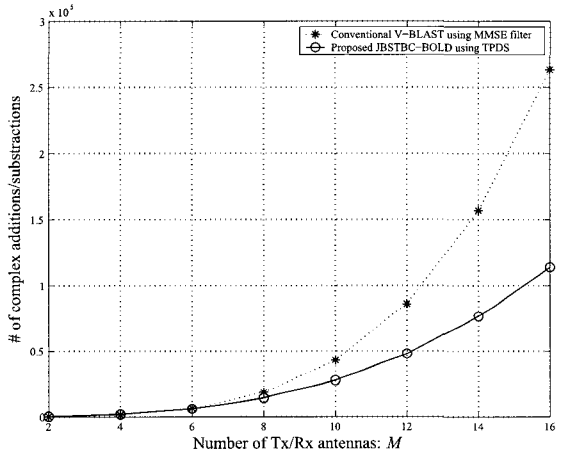

Fig. 14. Number of complex addtions/substractions vs number of Tx/Rx antennas.

of considerable inter-substream interferences. Therefore, in this situation, the rearrangement of transmit powers is desired for an effective discrimination so as to purposely enlarge the deviation of the received SINRs. Towards this, as explained in Section IV, the TPDS is performed via calculating extra weights for power allocation based on the proposed PDF with respect to the eigenvalues of transmit spatial covariance matrix.

Figs. 8 and 9 show the BER curves resulted from applying the proposed JBSTBC combined with BOLD as well as TPDS with varying symbol constellation. In order to validate the performance improvement, corresponding results are compared with those from the double STTD (D-STTD) method. Here, D-STTD method introduced in [5] is the one of open-loop style transmission schemes provided that corresponding receiver utilizes MRC only. As shown in Fig. 8, for QPSK case, the proposed JBSTBC method (in solid lines) in which TPDS is performed based on PDF having the CO of 3 outperforms D-STTD (in dotted lines) for any correlation condition. In Fig. 9, this trend is sustained even for 16-QAM case. Moreover, as discussed in Section IV, the usage of ad-hoc power allocation does not give rise to the performance benefit in the highly correlated situation, so that no further improvement is achieved as shown in Figs. 8 and 9. On the contrary, in the weakly correlated situation, the effect on the usage of TPDS is quite substantial as shown in Figs. 8 and 9, surely, this performance enhancement is attributed to the enforcement of power rearrangement based on the usage of PDF.

As mentioned in Section IV, since the exact formula for choosing optimal curve order is yet to be available, exhaustive simulation works as shown in Fig. 10 have been done for the intuitive choice of integer-valued CO instead. More specifically, by carrying out a series of trials with varying the curve order in integer value, the most plausible CO is selected among the candidates providing the most prominent BER behavior upon the prescribed constellation size. Clearly, Fig. 10 reinforces how to select the curve order in the case of QPSK modulation, which shows the BER curves obtained with varying the integer-valued curve order with respect to the specified E_b/N_0's. Here, the low correlated channel situation, i.e., Cases #3 and #4, is considered because relevant weighting value turns out to be almost unity for both Cases #1 and #2. Consequently, the CO is set to 3 and 6 for QPSK and 16-QAM, respectively. As a matter of fact, this approach is quite suboptimal, so that the closed form solution for the selection of optimal CO will be investigated as a future research.

Table 3. Comparison of computational complexity between V-BLAST and proposed JBSTBC-BOLD using TPDS.

V-BLAST using MMSE filter [28] one-step initialization and $(M-1)$ steps in the recursion			Proposed JBSTBC-BOLD using TPDS one-step initialization and $(M/2-1)$ steps in the recursion		
Item	Multiplications	Additions	Item	Multiplications	Additions
$[\mathbf{H}^H\mathbf{H}+\alpha\mathbf{I}_{M\times M}]^{-1}$	$9M^3+(4N+1)M^2$	$9M^3+(4N-1)M^2$	$\mathbf{W}$	$8M^3+5NM^2+1$	$8M^3+5NM^2-M^2$
$\tilde{s}=<\mathbf{Q}>_j \mathbf{H}^H\mathbf{y}$	$M(N+1)$	$M(N+1)-1$	$\mathbf{V}$	$8M^3+4NM^2+N^2M+1$	$8M^3+4NM^2+N^2M-N^2$
Nulling	N	N	$\Theta^H\Theta$	$2NM^2$	$2NM^2-M^2$
			$SINR_k$	$\frac{M^2}{2}+\frac{M}{2}$	$\frac{M}{2}-1$
			Nulling	$2M$	$2M$

Table 4. Total number of multiplications/additions.

	V-BLAST using MMSE filter [28]	Proposed JBSTBC-BOLD using TPDS
Total number of multiplications	$\frac{9}{4}M^4+\frac{4}{3}M^3N+\frac{29}{6}M^3+\frac{5}{2}M^2N+\frac{13}{4}M^2+\frac{13}{6}MN+\frac{2}{3}M-N$	$\frac{769}{48}M^3+11M^2N+\frac{1}{4}M^2+MN^2-\frac{19}{12}M+3$
Total number of additions	$\frac{9}{4}M^4+\frac{4}{3}M^3N+\frac{25}{6}M^3+\frac{5}{2}M^2N+\frac{9}{4}M^2+\frac{13}{6}MN-\frac{2}{3}M-N$	$16M^3+11M^2N-\frac{27}{16}M^2+MN^2-\frac{17}{8}M-N^2+3$

Although the above comparative work exploits the degree of goodness in BER behavior of the proposed method in closed-loop style against D-STTD scheme in open-loop style, the results seems to be unfair because only the proposed scheme utilizes CSI in a form of covariance feedback. In order to verify the performance from another point of view, our proposed method, i.e., JBSTBC combined with BOLD as well as TPDS, is compared with the scheme employing either the conventional OSTBC [4] combined with EBF as well as waterfilling in the notion of the optimal precoding on the basis of covariance feedback [15].

Referring to the results in Figs. 8 and 9, since the performance of the proposed TPDS is surely effective in the existence of relatively weak correlation between channels, the comparative works are accomplished only for Cases #3 and #4. Here, for the sake of fair comparison, considering the different code rate between the proposed and OSTBC, the code rate of OSTBC is presumed to be 1/2. Thus, if the symbol constellation of the proposed is set to be QPSK and 16-QAM, corresponding symbol constellation of OSTBC is 16-QAM and 256-QAM, respectively. As can be clearly seen in Figs. 11 and 12, the proposed method is superior in the aspect of BER behavior to OSTBC employing linear precoder comprised of EBF and waterfilling [15].

According to the generic structure as shown in Fig. 1, since the proposed transmitter sends spatially multiplexed STBC-coded substreams, the corresponding receiver could employ MMSE- or ZF-type of linear filtering right after the STBC decoding process. For executing these receiving algorithms, a series of matrix inversions should be involved along the LSIC based on a priori estimated channel parameters. As mentioned earlier in this section, the amount of computations becomes enormous as the number of receiving antennas is increased. For further investigation, Tables 3 and 4 reveals the amount of computational complexity as the number of complex multipliers as a function of the number of transmit and receive antennas.

More specifically, Table 3 contains the required number of complex multipliers corresponding to major functionalities associated with V-BLAST receiver employing MMSE filtering [25], [26], [28] as well as the proposed JBSTBC-BOLD receiver discussed in Section IV. In Table 3, the complexity for finding items $\mathbf{W}$ and $\mathbf{V}$ counts the computations relevant to the update of transmit and receive covariance matrices as well as corresponding eigenvectors and eigenvalues. Assuming that the feedback CSI comprises of the eigenvectors and associated eigenvalues associated to transmit covariance matrix, the complexity for obtaining transmit EBF is also taken into account. And the overall numbers of complex multipliers needed for V-BLAST receiver and the proposed JBSTBC-BOLD are shown in Table 4, and Figs. 13 and 14 show the amount of complex multiplications provided that the number of transmit antennas is the same as that of receive antennas designated as M. As can be obviously seen in Figs. 13 and 14, the proposed JBSTBC-BOLD receiver demands less number of multiplications, and the corresponding gap becomes aggravated as the number of antennas is increased.

VI. CONCLUSION

This paper proposed a novel MIMO system designated as JBSTBC, which is comprising of eigen-beamformers at both transmitter and receiver, space-time block encoder/decoder, and TPDS based on PDF at transmitter and BOLD at receiver. Along the recovery of spatially multiplexed substreams, a series of LSICs incorporating with simple MRC are conducted in sequence based on the determination of the priority of detection order. However, when fading channels are weakly correlated, a performance degradation is encountered inevitably because of the imperfect interference cancellation. In order to circumvent this deterioration, this paper proposed a suboptimal power allocation accomplished via performing the proposed TPDS with the help of the PDF parameterized in terms of the ESR and the CO. The superior performance of the proposed scheme in the aspect of BER behavior as well as computational complexity was confirmed by conducting many comparative simulation works. Hereafter, the author will pursue more extensive and analytic works throughout the theoretical development to show the superiority in error rate performance and achievable transmission rate upon either perfect or imperfect covariance feedback. Moreover, since the parameter CO is selected in suboptimal manner in this paper, as another future work, a proper crite-

rion will be formulated so as to exploit the exact closed-form for choosing optimum parameter CO.

ACKNOWLEDGEMENT

This work was supported by HY-SDR Research Center at Hanyang University, Seoul, Korea, under the ITRC Program of MIC, Korea, and the Soongsil University Research Fund.

REFERENCES

[1] G. J. Foschini, "Layered space-time architecture for wireless communication in fading environment when using multi-element antennas," *Bell Labs Tech. J.*, pp. 41–59, Autumn 1996.
[2] E. Viterbo and J. Boutros, "A universal lattice code decoder for fading channel," *IEEE Trans. Inform. Theory*, vol. 45, pp. 1639–1642, July 1999.
[3] S. Zhou and G. B. Giannakis, "Optimal transmitter eigen-beamforming and space-time block coding based on channel mean feedback," *IEEE Trans. Signal Processing*, vol. 50, no. 10, pp. 2599–2613, Oct. 2002.
[4] V. Tarokh, H. Jafarkhani, and and A. R. Calderbank, "Space-time block coding for wirless communications: Performance results," *IEEE J. Select. Areas Commun.*, vol. 17, no. 3, pp. 451–460, Mar. 1999.
[5] E. N. Onggosanusi, A. G. Dabak, and T. M. Schmidl, "High rate space-time block coded scheme: Performance and improvement in correlated fading channels," in *Proc. WCNC 2002*, vol. 1, Florida, USA, Mar. 2002, pp. 194–199.
[6] H. Wang, and X. Xia, "Upper bounds of rates of complex orthogonal space-time block codes," *IEEE Trans. Inform. Theory*, vol. 49, no. 10, pp. 2788–2796, Oct. 2003.
[7] H. Jafarkhani, "A quasi-orthogonal space-time block code," *IEEE Trans. Commun.*, vol. 49, no. 1, pp. 1–4, Jan. 2001.
[8] L. He and H. Ge, "A new full-rate full-diversity orthogonal space-time block coding scheme," *IEEE Commun. Lett.*, vol. 7, no. 12, pp. 590–592, Dec. 2003.
[9] H. El Gamal, "On the robustness of space-time coding," *IEEE Trans. Signal Processsing*, vol. 50, pp. 2417–2428, Oct. 2002.
[10] D. Chizhik, F. Rashid-Farrokhi, J. Ling, and A. Lozano, "Effect of antenna separation on the capacity of BLAST in correlated channels," *IEEE Commun. Lett.*,vol. 4, no. 11, pp. 337–339, Nov. 2000.
[11] J. M. Kahn, C. Chuah, and D. Tse, "Capacity of multi-antenna array systems in indoor wireless environment," in *Proc. GLOBECOM'98*, 1998.
[12] D-S. Shiu, G. J. Foschini, M. J. Gans, and J. M. Kahn, "Fading correlation, and its effect on the capacity of multielement antenna systems," *IEEE Trans. Commun.*, vol. 48, no. 3, pp. 502–513, Mar. 2000.
[13] M. Ivrlac, T. Kurpjuhn, C. Brunner, and W. Utschick, "Efficient use of fading correlations in MIMO systems," in *Proc. VTC 2001-fall*, vol. 4, Atlantic City, USA, Oct. 2001, pp. 2763–2767.
[14] T. Kurpjuhn, M. Joham, W. Utschick, and J. Nossek, "Experimental studies about eigenbeamforming in standardization MIMO channels," *Proc. VTC 2002-fall*, vol. 1, Vancouver, Canada, Sept. 2002, pp. 185–189.
[15] Y. Zhao, R. Adve, and T. J. Lim, "Precoding of orthogonal STBC with channel covariance feedback for minimum error probability," in *Proc. IEEE PIMRC 2004*, vol. 1, Sept. 2004, pp. 503–507.
[16] S. Jafar, S. Vishwanath, and A. Goldsmith, "Channel capacity and beamforming for multiple transmit and receive antennas with covariance feedback," in *Proc. IEEE ICC 2001*, vol. 7, Helshinki, Filand, June 2001, pp. 2266–2270.
[17] H. Sampath and A. Paulraj, "Linear precoding for space-time coded systems with known fading correlations," *IEEE Commun. Lett.*, vol. 6, no. 6, pp. 239–241, June 2002.
[18] G. Jongren, M. Skoglund, and B. Ottersten, "Combining beamforming and orthogonal space-time block coding," *IEEE Trans. Inform. Theory*, vol. 48, no. 3, pp. 611–627, Mar. 2002.
[19] D. J. Love and R. W. Heath, "Limited feedback unitary precoding for spatial multiplexing systems," *IEEE Trans. Inform. Theory*, vol. 51, no. 8, pp. 2967–2976, Aug. 2005.
[20] J. Akhtar, "Diversity and spatial-multiplexing tradeoff under linear decoding," in *Proc. IEEE VTC 2004-spring*, vol. 2, May 2004, pp. 589–593.
[21] "Further link level results for HSDPA using multiple antennas," 3GPP TSG RAN WG1 TSGR1#17(00)1386, 12-24-th, Stockholm, Sweden, Nov. 2000.
[22] D. Chizhik, J. Ling, P. Wolniansky, R. Valenzuela, N. Costa, and K. Huber, "Multiple input multiple output measurements and modeling in mahattan," in *Proc. VTC 2002-fall*, vol. 1, Vancouver, Canada, Sept. 2002, pp. 107–110.
[23] "Discussion on the MIMO Channel Model," 3GPP TSG RAN WG1 TSGR#Rel5(01)0702, June 2001.
[24] "Double-STTD scheme for HSDPA systems with four transmit antennas: Link level simulation," 3GPP TSG RAN TSGR1#20(01)0458, 2001.
[25] P. W. Wolniansky, G. J. Foschini, G. D. Golden, and R. A. Valenzuela, "V-BLAST: An architecture for realizing very high data rates over the rich-scattering wireless channel," in *Proc. ISSSE'98*, Pisa, Italy, 1998.
[26] G. D. Golden, C. J. Foschini, R. A. Valenzuela, and P. W. Wolniansky, "Detection algorithm and initial laboratory results using V-BLAST space-time communication architecture," *IEE Electron. Lett.*, vol. 35, no. 1, pp. 14–16, Jan. 1999.
[27] "A standardized set of MIMO radio propagation channels," 3GPP TSG RAN WG1#23(01)1179, Nov. 2001.
[28] J. Benesty, Y. Huang, and J. Chen, "A fast recursive algorithm for optimum sequential signal detection in a BLAST system," *IEEE Trans. Signal Processing*, vol. 51, no. 7, July 2003.

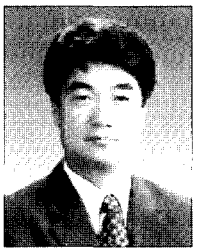

Won Cheol Lee was born in Seoul, Korea, on December 26, 1963. He received his B.S. degree in Electronic Engineering from Sogang University in 1986 and M.S. degree from Yonsei University and Ph.D. degree from Polytechnic University, New York, in 1988, 1994, respectively. He joined Polytechnic University as a Post-Doctoral Fellow from July 1994 to July 1995. He has been an Associate Professor of School of Electronic Engineering, Soongsil University since September 1995. From July 1999 to November 1999, he was a visiting researcher at ETRI. He has been working in the HY-ITRC of Hanyang University on software defined radio as a researcher since July 2002. His research area includes cognitive radio, ultra wideband radio system, space-time signal processing, and software defined radio. He is a member of IEEE, IEICE, IEEK, KICS, and Sigma Xi.